Dynamics of Atmospheres and Oceans 83 (2018) 53–63

Contents lists available at ScienceDirect

Dynamics of Atmospheres and Oceans

journal homepage: www.elsevier.com/locate/dynatmoce

Evaluation of regional climate models performance in simulating rainfall climatology of Jemma sub-basin, Upper Blue Nile Basin, Ethiopia

Gebrekidan Worku[a,*], Ermias Teferi[a], Amare Bantider[b,c], Yihun T. Dile[d], Meron Teferi Taye[c]

[a] Center for Environment and Development Studies, Addis Ababa University, Ethiopia
[b] Center for Food Security Studies, Addis Ababa University, Ethiopia
[c] Water and Land Resources Centre, Addis Ababa University, Ethiopia
[d] College of Agriculture and Life Sciences, Texas A&M University, TX, USA

ARTICLE INFO

Keywords:
Regional Climate Models
Downscaling
RCM evaluation
Rainfall
Upper Blue Nile

ABSTRACT

This study examines the performance of 10 Regional Climate Model (RCM) outputs which are dynamically downscaled from the fifth phase of Coupled Model Inter-comparison Project (CMIP5) GCMs using different RCMs parameterization approaches. The RCMs are evaluated based on their ability to reproduce the magnitude and pattern of monthly and annual rainfall, characteristics of rainfall events and variability related to Sea Surface Temperature (SST) for the period 1981–2005. The outputs of all RCMs showed wet bias, particularly in the higher elevation areas of the sub-basin. Wet bias of annual rainfall ranges from 9.60% in CCLM4 (HadGEM2-ES) model to 110.9% in RCA4 (EC-EARTH) model. JJAS (June-September) rainfall is also characterized by wet bias ranges from 0.76% in REMO (MPI-ESM-LR) model to 100.7% in RCA4 (HadGEM2-ES) model. GCMs that were dynamically downscaled through REMO (Max Planck Institute) and CCLM4 (Climate Limited-Area Modeling) performed better in capturing the rainfall climatology and distribution of rainfall events. However, GCMs dynamically downscaled using RCA4 (SMHI Rossby Center Regional Atmospheric Model) were characterized by overestimation and there are more extreme rainfall events in the cumulative distribution. Most of the RCMs' rainfall over the sub-basin showed a teleconnection with Sea Surface Temperature (SST) of CMIP5 GCMs in the Pacific and Indian Oceans, but weak. The ensemble mean of all 10 RCMs simulations was superior in capturing the seasonal pattern of the rainfall and had better correlation with observed annual (Correl = 0.6) and JJAS season rainfall (Correl = 0.5) than any single model (S-RCM). We recommend using GCMs downscaled using REMO and CCLM4 RCMs and stations based statistical bias correction to manage elevation based biases of RCMs in the Upper Blue Nile Basin, specifically in the Jemma sub-basin.

1. Introduction

Global Climate Models (GCMs) are instrumental to assess relative change in the climate system due to various radiative forcing and make climate predictions on seasonal to decadal time scales and projections of future climate (IPCC, 2013). Many GCMs were

* Corresponding author.
E-mail address: kidanw1@gmail.com (G. Worku).

https://doi.org/10.1016/j.dynatmoce.2018.06.002
Received 21 October 2017; Received in revised form 12 June 2018; Accepted 13 June 2018
Available online 15 June 2018
0377-0265/ © 2018 Elsevier B.V. All rights reserved.

developed by different climate research centers since the 1950 s (Edwards, 2010). The establishment of the Earth System Modeling Framework (ESMF) which couples atmosphere–ocean GCMs with the land surface, the cryosphere, hydrology and vegetation processes is another framework in climate modeling (Hill et al., 2009). Despite improvements in the GCMs, challenges remain on their spatial resolution and parameterization. GCMs' rainfall simulation at the national and regional scales remains difficult (Randall et al., 2007; Flato et al., 2013). Moreover, GCMs that have coarse spatial resolutions could not realistically capture climatic extreme events. Particularly, in regions where there is an uneven topography, downscaling climate models at regional spatial scale is vital to get accurate information for local climate impact studies (Flato et al., 2013).

Regional Climate Models (RCMs) are developed with higher spatial resolution to describe climate variability at regional scale. RCMs add value compared to GCMs in simulating climate of coastal and mountainous regions and in mesoscale (i.e. a spatial scale of 1–100 km) (Giorgi et al., 2009; Feser et al., 2011). There are different initiatives to produce large ensembles of RCM simulations that can be further used for climate change impact assessment at regional spatial scales. CORDEX (Coordinated Regional Climate Downscaling Experiment) under the auspices of the World Climate Research Program (WCRP) is an initiative to downscale different GCM outputs that participated in the Coupled Model Inter-comparison Project Phase 5 (CMIP5) and to generate an ensemble of high-resolution historical and future climate projections for the African continent (Giorgi et al., 2009; Taylor et al., 2012). CORDEX simulations add value over GCMs in Africa, particularly in representing the annual cycle of rainfall and extreme rainfall events in different regions of the continent (Nikulin et al., 2012; Dosio et al., 2015; Kim et al., 2014). However, uncertainty persists in RCMs' simulation of rainfall, temperature, wind and other processes (Varis et al., 2004). Distinguishing the cause of uncertainty is difficult since it may come from either the initial boundary conditions (GCM) or RCMs parameterization. The other problem of RCMs is their inconsistency of performance across regions and seasons (Gleckler et al., 2008; Feser et al., 2011; Endris et al., 2013) which warrants caution in choosing RCMs to study a particular region and/or seasons.

Different studies evaluated the performance of climate models representing the climate of the Upper Blue Nile Basin using various techniques (e.g. Bhattacharjee and Zaitchi, 2015; Jury, 2015; Haile and Rientjes, 2015). Most of these studies compared observed and model outputs and evaluated the ability of climate models in capturing inter-annual variability associated with natural climate processes such as El Niño-Southern Oscillation (ENSO) (Bhattacharjee and Zaitchi, 2015; Jury, 2015; Haile and Rientjes, 2015). Little consistency was found in the performance of model outputs in simulating amount and seasonality of rainfall, and teleconnections across the Nile River headwaters region (Bhattacharjee and Zaitchi, 2015). The difference in the performance of climate models in capturing annual cycle and inter-annual variability of rainfall and maximum temperature was also studied in the Blue Nile region of Ethiopia (Jury, 2015).

Uncertainty in climate model outputs for climate change impact assessment can be reduced using multiple lateral boundary conditions (GCMs), multiple RCM outputs, and robust downscaling methods (Feser et al., 2011; Flato et al., 2013; USAID, 2014). However, only limited studies consider diversity of methods and climate model outputs to show the range of uncertainty. For example, in the Upper Blue Nile Basin, only a couple of studies used multiple GCM outputs and multiple RCM simulations (Haile and Rientjes, 2015; Endris et al., 2013; Bhattacharjee and Zaitchi, 2015; Nikulin et al., 2012). In fact, most of these studies used limited RCMs downscaled using few numbers of initial boundary condition (GCMs). For example, Dosio et al (2015) has analyzed the added value of four GCMs downscaled by single RCM (COnsortium for Small-scale MOdeling, COSMO-CCLM). Haile and Rientjes (2015) evaluated the performance of eight GCMs downscaled using single RCM (RCA4) in the Blue Nile Basin. While other studies used reanalysis datasets than observational data sets to evaluate RCMs (Endris et al., 2013; Bhattacharjee and Zaitchi, 2015) which are characterized by biases in estimating rainfall (Nikulin et al., 2012).

The objective of this study is to evaluate the performance of multiple RCMs driven by multiple GCMs in capturing the mean annual and monthly rainfall, distribution of rainfall events and large-scale climate circulation patterns (teleconnections) in the Jemma sub-basin, Upper Blue Nile Basin for the period 1981–2005. Observed data collected from the Ethiopian National Meteorological Agency (NMA) was used for evaluation. The RCMs which capture rainfall climatology of the Jemma sub-basin will be used for further statistical bias correction, hydrological modeling, and other climate change mitigation and adaptation measures in the sub-basin.

2. Materials and methods

2.1. Description of the study area

This study was conducted in the Jemma sub-basin, which is one of the sub-basins of the Upper Blue Nile Basin. It is located in the Central Highland of Ethiopia (Fig. 1), whose climate is highly influenced by moisture coming from the Indian Ocean, Equatorial east Pacific, Gulf of Guinea, Mediterranean region and Arabian Peninsula (Seleshi and Zanke, 2004; Viste and Sorteberg, 2011). The sub-basin has a catchment area of ~15,000 km^2, which accounts ~8% of the area and ~14% of the flow of the Upper Blue Nile Basin (Yilma and Awulachew, 2009). Jemma sub-basin is highly prone to soil erosion; the long-term average annual sediment yield at the sub-basin outlet is 21.2 million tons (Ali et al., 2014). The elevation in the sub-basin ranges from 1040 m to 3814 m above sea level.

Jemma sub-basin receives annual rainfall ranges between 697 mm to 1475 mm. The sub-basin has two rainfall seasons. JJAS (i.e. June- September) locally called *Kiremt*is the main rainfall season followed by spring season (March-May) (MAM)) locally called *Belg*. Mean annual temperature in the sub-basin ranges from 9 °C to 24 °C. The agro-ecologies in the sub-basin range from cold, moist sub-Afro alpine to warm sub-moist lowlands (MoA, 2000).

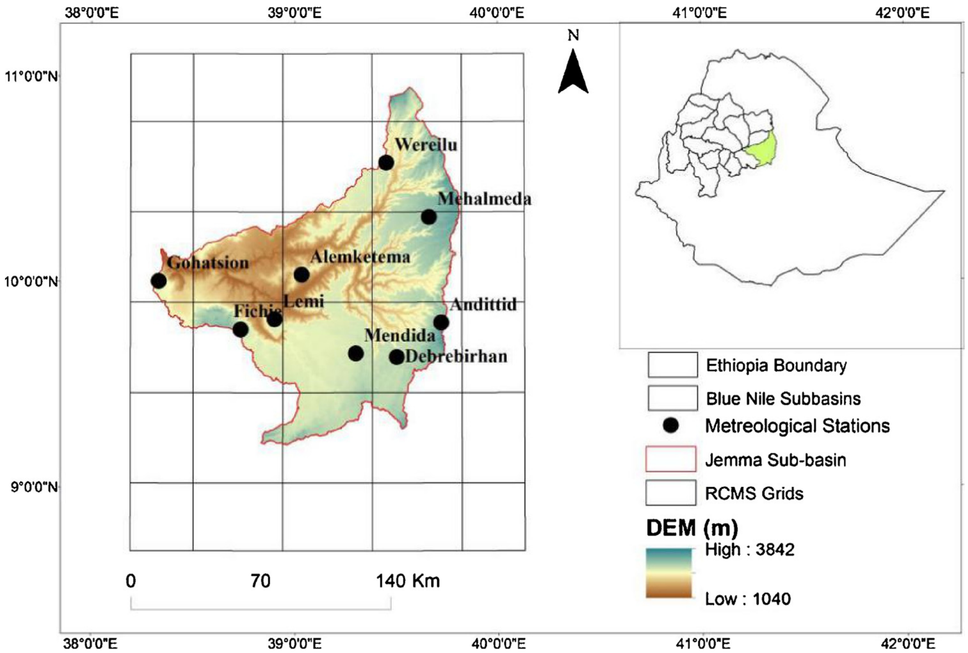

Fig. 1. Grids of Regional Climate Models and distribution of meteorological stations over Jemma sub-basin.

2.2. Data and methods

2.2.1. Observed data

Daily observed rainfall data for the period 1981–2005 was used for regional climate models evaluation. The observed data for nine climatic stations located within the Jemma sub-basin was collected from NMA. The missing data were completed using Multivariate Imputation by Chained Equations (MICE) algorithm (Buuren et al., 2015), which is available on R statistical software (R Development Core Team, 2015). The MICE algorithm calculates missing values at a single station using the complete observed values of all stations under study as predictors. The MICE creates multiple predictions for each missing value and considers uncertainty in the calculations and provides standard errors (Buuren et al., 2015). As such, the MICE algorithm is better than other methods such as inverse distance weighting (IDW) and multiple linear regression (MLR) in completing missing data (Turrado et al., 2014).

The quality of observed data of all stations was examined using RClimDex 1.1 (Zhang and Yang, 2004). Errors such as minimum temperature greater than maximum temperature, and negative rainfall values were corrected using the nearby stations. Outlier values (i.e. data which are outside mean $\pm$ four times the standard deviation) were changed into average values of days before and after the outliers' day (WMO, 2009). The observed data after the quality control was used for this study.

2.2.2. RCMs data

Historical RCM simulation outputs (1981–2005) driven by four CMIP5 GCMs were used in this study. The GCMs which were used as initial boundary conditions were CNRM-CM5, EC-EARTH, HadGEM2-ES and MPI-ESM-LR (Table 1). The historical simulations of these GCMs were initialized with the atmosphere, ocean, land and sea surface temperature (SST) conditions and forced by observed natural and anthropogenic CO_2 and aerosol concentrations (Taylor et al., 2012). The RCMs used to regionalize these GCMs were the COnsortium for Small-scale MOdeling (COSMO) Climate Limited-Area Model (CCLM) version 4.8, Rossby Centre Regional Climate Model (RCA4) and Max Planck Institute Regional Model (REMO) (Table 2). These RCMs were selected for evaluation since they (especially CCLM and RCA models) were used to downscale historical and future simulations of multiple CMIP5 GCMs (e.g. CNRM-CM5, EC-EARTH, HadGEM2-ES, and MPI-ESM-LR) in the CORDEX project. The outputs of CCLM4 and RCA4 RCMs driven by these four GCMs were frequently evaluated and showed reasonable performance over Africa (Nikulin et al., 2012; Dosio et al., 2015; Kim et al., 2014). Both rainfall and SST data of models were obtained from the publicly available Earth System Grid Federation (ESGF)

Table 1
Global Climate Models (drivers) considered in this study.

GCM	Institute	Country
CNRM-CM5	CNRM–CERFACS: Centre National de Recherches Météorologiques	France
EC-EARTH	ICHEC: Consortium of European research institutions and researchers	Europe
HadGEM2-ES	MOHC: Met Office Hadley Centre	United Kingdom
MPI-ESM-LR	MPI-M: Max-Planck-Institute	Germany

Table 2
Description of Regional Climate Models considered in this study.

RCM	Full Name	Institute	Reference
CCLM	CLMcom COSMO-CLM (CCLM) version 4.8	Climate Limited-Area Modelling (CLM) Community (www. clm-community.eu)	Baldauf et al. (2011)
RCA4	SMHI Rossby Center Regional Atmospheric Model (RCA4)	Sveriges Meteorologiska och Hydrologiska Institut (SMHI), Sweden	Samuelsson et al. (2011)
REMO	MPI regional model (REMO)	Max Planck Institute (MPI), Germany	Jacob et al. (2007)

web portals.

RCMs' rainfall values which were obtained from grids fully or partially cover the Jemma sub-basin (Fig. 1). For each model, 'historical' simulations and only the first ensemble member (r1) was used, except the EC-EARTH model from which the 12th ensemble member (r12) was used. The outputs of these simulations were obtained at a resolution of ~50 km by 50 km from the Africa domain CORDEX dataset. Overall, this study used 10 RCM outputs which were downscaled from four GCMs using three RCMs (only EC-EARTH and MPI-ESM-LR downscaled through REMO are considered). The ensemble mean of these 10 RCMs was also used for the evaluation.

The observed rainfall data (point data) which is collected from meteorological stations was converted into spatial data. This is to match with RCMs gridded data. Thiessen Polygon method (Theissen, 1911) was used to split the sub-basin into smaller polygons based on area of influence of location of observation stations and to calculate areal rainfall. The Thiessen Polygon method calculates areal rainfall (sub-basin wide rainfall) to each Thiessen Polygon based on the area of the polygon in proportion to the total area of the sub-basin. Similarly, Thiessen Polygon method was used to estimate rainfall of each RCM in the entire sub-basin based on the area of the RCMs' grids fully or partially covering the Jemma sub-basin (Fig. 1). After the observed and RCMs data were converted into area-average (spatial) rainfall, different metrics were used to evaluate RCMs performance in simulating the rainfall of the Jemma sub-basin.

2.2.3. Methods

Three criteria were used to measure performance of climate models in simulating rainfall of the study area. The first criterion assesses the ability of the RCMs to reproduce the rainfall climatology and characteristic of rainfall events. This criterion compared the magnitude of mean annual and seasonal rainfall, mean monthly rainfall pattern, distribution and frequency of rainfall events and return period of RCMs outputs to that of the observed data.

The second evaluation uses statistical metrics, including BIAS, Root Mean Squared Error (RMSE) and Correlation Coefficient (Correl) between areal averaged rainfall of RCMs and observation.

$$Correl = \frac{\sum_{t=1}^{N}(R_{RCM} - \overline{R_{RCM}})(R_{Observ} - \overline{R_{Observ}})}{\sqrt{\sum_{t=1}^{N}(R_{RCM} - \overline{R_{RCM}})\sum_{t=1}^{N}(R_{Observ} - \overline{R_{Observ}})}}$$

$$\mathrm{BIAS} = 100^{*}\frac{\overline{\mathrm{R_{RCM}} - \mathrm{R_{Observ}}}}{\mathrm{R_{Observ}}}$$

$$\mathrm{RMSE} = \sqrt{\frac{1}{N}\sum_{i=1}^{N}(R_{RCM} - R_{Observ})^2}$$

Where, $\mathrm{R_{RCM}}$ is a rainfall of RCMs, $\mathrm{R_{Observ}}$ is a rainfall of stations, the bar over the variables denotes the average over a period of 1981–2005, and N represents the analysis period (25 years).

The correlation is often used to evaluate the linear relationship between areal averaged RCM rainfall and observed rainfall. Values close to 1.0 indicate a better linear relationship between the variables and a value away from 1.0 indicates less agreement. BIAS is used to measure the volumetric difference between the RCM rainfall and observed rainfall. A BIAS value close to 0 indicates a minor systematic difference between RCM rainfall and observed rainfall amounts, whereas a BIAS value far from 0 suggests a deviation. RMSE measures the difference between RCM rainfall and observed rainfall. An RMSE value close to zero indicates better performance.

The third criterion evaluates the teleconnection between Sea Surface Temperature (SST) of CMIP5 GCMs in the Pacific and Indian Oceans and rainfall simulated by RCMs over the Jemma sub-basin. Since RCMs cover only a particular domain, we are not able to get SST data simulated by RCMs over different oceanic regions. As a result, SST of parent GCM and rainfall of RCMs is used to compute SST-rainfall teleconnection. SST of the equatorial Pacific and Indian Oceans are drivers of rainfall of the central highlands of Ethiopia and the study region (Gissila et al., 2004; Diro et al., 2011; Rowell, 2013). NINO3.4 index is considered to analyze GCMs simulation of SST anomaly over the Pacific Ocean. NINO3.4 index is the average SST over the region 5 °S–5 °N, 170 °E–120 °W (Rowell, 2013; Endris et al., 2016). While, Indian Ocean Dipole (IOD) is considered to analyze GCMs simulation of SST anomaly over the Indian ocean. Indian Ocean Dipole (IOD) is the difference in the average SST of West Indian Ocean (IODW) over the region 10 °S–10 °N, 50 °E–70 °E) and East Indian Ocean (IODE) over the region 10 °S–0 °N, 90 °E–110 °E (Saji et al., 1999; Gissila et al., 2004; Rowell,

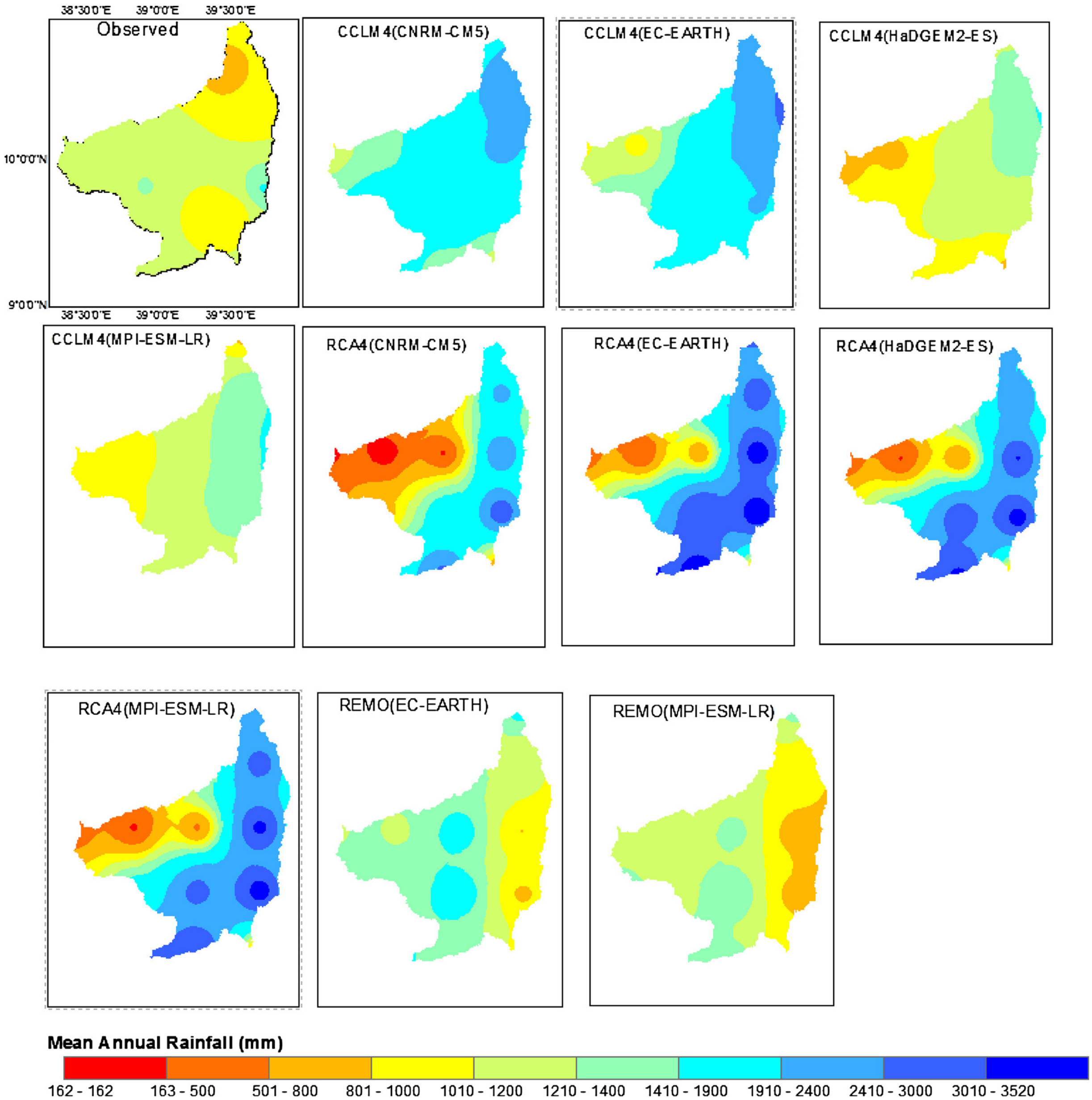

Fig. 2. Long-term (1981–2005) mean annual rainfall from the observations and regional climate models.

2013; Endris et al., 2016).

3. Results and discussion

3.1. Rainfall climatology

Annual, seasonal, and monthly rainfall amount and distribution of rainfall events simulated by different RCMs for the period 1981–2005 showed a clear difference between the models. Fig. 2 shows long term (1981–2005) average annual rainfall of different RCMs and observation stations. REMO model outputs were better in representing observed annual rainfall compared to other models. REMO model outputs were higher than observed rainfall in the middle and lower regions of the sub-basin. GCMs data downscaled using RCA4 model showed a weak performance in capturing annual rainfall of the Jemma sub-basin. Outputs from RCA4 model were characterized by underestimation in the lower altitudes and overestimation in the higher altitudes. GCMs downscaled using CCLM4 model also showed overestimation in the higher altitudes of the Jemma sub-basin (Fig. 3). Similar to this study, Endris et al. (2013) and Zaroug et al. (2014) showed that CCLM4, RCA4 and RegCM3 model outputs overestimate rainfall over the Ethiopian highlands

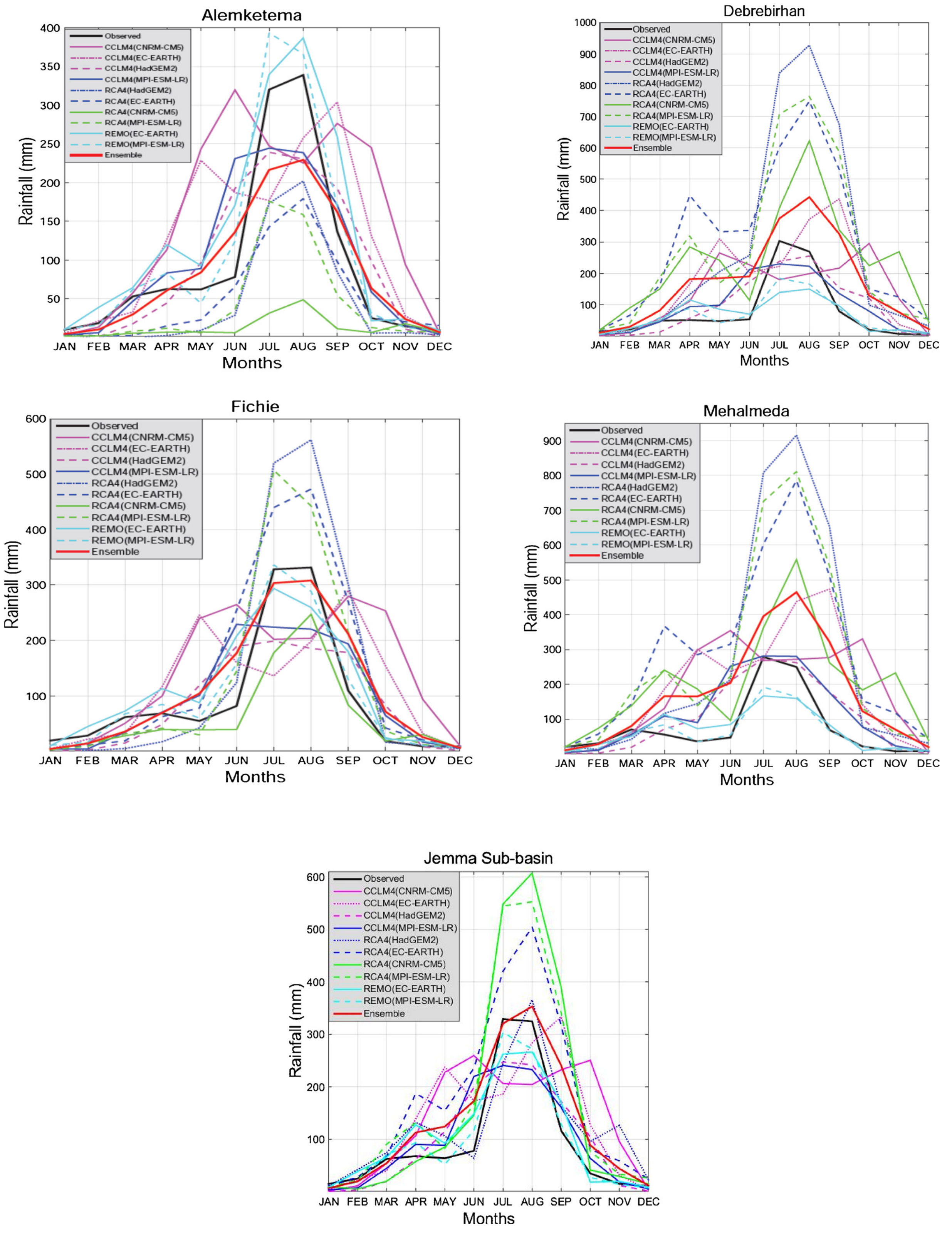

Fig. 3. Long-term (1981–2005) mean monthly rainfall from the observations and regional climate models at different stations and in the entire Jemma sub-basin. The rainfall of the entire jemma sub-basin is areal rainfall of observation and Regional Climate Models.

than other regions of East Africa. Kim et al. (2014) found that CCLM4, RCA4 and REMO models driven by ERA-Interim reanalysis overestimate rainfall in the highlands of Ethiopia. Haile and Rientjes (2015) also reported positive bias of RCMs in the high altitude areas of the Upper Blue Nile Basin.

Most of the models captured monthly pattern of rainfall of individual stations and areal-averaged rainfall (Fig. 3). High amount of rainfall is simulated in JJAS season, where notable inter-model differences in simulating magnitude of monthly rainfall were observed. REMO models were superior in capturing the monthly pattern of observed rainfall, while models outputs downscaled by RCA4 RCM showed the poorest performance in capturing monthly rainfall distribution. GCMs downscaled by RCA4 overestimated JJAS season rainfall at stations of higher altitude (e.g. Debrebirhan and Mehalmeda stations) and underestimated at stations of lower altitude (e.g. Alemketema). Herna′ndez-Diaz et al. (2013) also showed overestimation of JJAS season rainfall over the Ethiopian Highlands for the period 1984–2008 using CRCM5 (Canadian Regional Climate Model) driven by ERA reanalysis. Area-averaged observed and RCMs′ rainfall values showed lower deviation in the pattern of monthly rainfall (Fig. 3). CCLM4, RCA4 and REMO driven by ERA-Interim reanalysis were among the models which realistically simulate JJAS season rainfall of the Ethiopian highlands (Endris et al., 2013).

3.2. Characteristics of rainfall events in regional climate models

The evaluation of RCMs in capturing distribution of extreme rainfall events is important since these extremes are responsible for flood and drought occurrences. There are a large number of dry days (0 mm/day) in the observed rainfall and RCMs rainfall. In both of the rainfall data, dry day events were observed mainly during winter and MAM seasons. More number of drizzle rainfall events (i.e. amount of rainfall < 0.1–0.9 mm/day) were simulated in all RCMs (except RCA4 (HadGEM2-ES) compared to observed rainfall. The drizzle rainfall events in RCM simulations were observed during winter and MAM seasons. Frequency of dry days is low in RCMs ensemble mean than individual RCMs, because the mean of drizzle rainfall in individual RCMs resulted non-zero values in the ensemble mean. Comparable frequency of rainfall events (1 mm–6 mm/day) was observed between observed and RCMs' ensemble mean (Fig. 4).

Similar to the observed rainfall frequency distribution (Fig. 4), there were more number of days with rainfall amount in the range of 0.5–10 mm/day in CCLM4 model family (CCLM4 (CNRM-CM5), CCLM4 (HadGEM2-ES), CCLM4 (EC-EARTH) and CCLM4 (MPI-ESM-LR) and REMO model family (REMO (EC-EARTH) and REMO (MPI-ESM-LR)). Dosio et al. (2015) evaluated outputs of four GCMs (MPI-ESM-LR, HadGEM2-ES, CNRM-CM5 and EC-EARTH) downscaled through CCLM4 and showed that these models were able to reproduce the distribution of rainfall and some extreme rainfall events over the entire Africa. RCMs simulations (especially RCA4 model family) had a higher number of heavy and very heavy rainfall events (10 mm–20 mm/day respectively (WMO, 2009)) than observed rainfall. Consistent with this study, using GCMs downscaled by RCA4, Haile and Rientjes (2015) reported high frequency of heavy rainfall events (10 mm/day) in the Upper Blue Nile Basin of Ethiopia.

Cumulative distribution of rainfall of RCMs showed clear inter-model difference in simulation of heavy rainfall events. The CCLM4 model family better reproduced the distribution of observed rainfall compared to other models (Fig. 5). The proportion of heavy rainfall (rainfall more than 10 mm/day) and very heavy rainfall (rainfall more than 20 mm/day) was about 40% and 10%, respectively in most RCA4 models. In contrast, the proportion of 10 mm/day rainfall was only about 10% in most of CCLM4 and REMO models as well as in the observed rainfall. In all models except RCA4 (EC-EARTH), the proportion of drizzle and light rainfall events (0.20–5 mm/day) account about 50% of the total rainfall (Fig. 5).

Similar to the cumulative distribution of rainfall events, all models overestimated the return period, especially RCA4 model family showed higher overestimation of the return period. REMO model family captured annual and JJAS return period of observed rainfall better than other models. In most RCA4 models, a return period of 25 years was estimated for 2500 mm/year rainfall, which is 150% higher than observed rainfall (Fig. 6). The annual and JJAS rainfall return period analysis (Fig. 6a and b) indicated that a large proportion of the annual rainfall (about 80%) was concentrated in the JJAS season. In few high altitude stations, RCA4 models

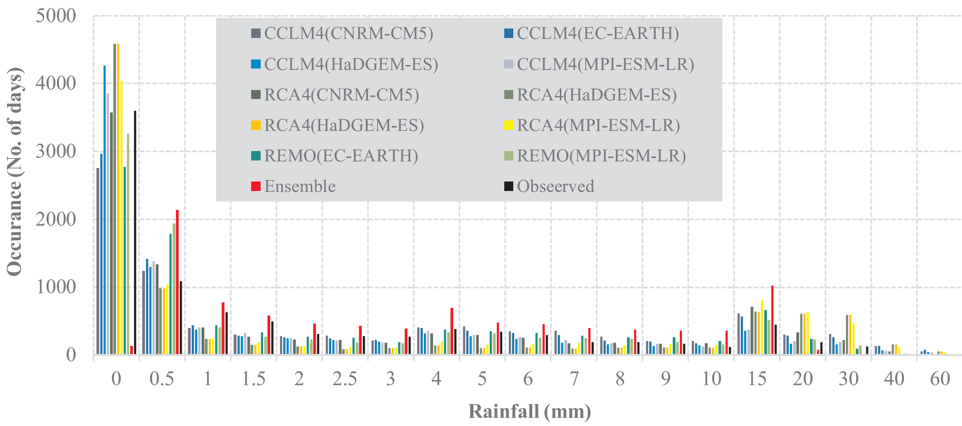

Fig. 4. Histogram of RCMs and Observational Daily Rainfall (1981–2005). The values of both observed and RCMs are areal rainfall.

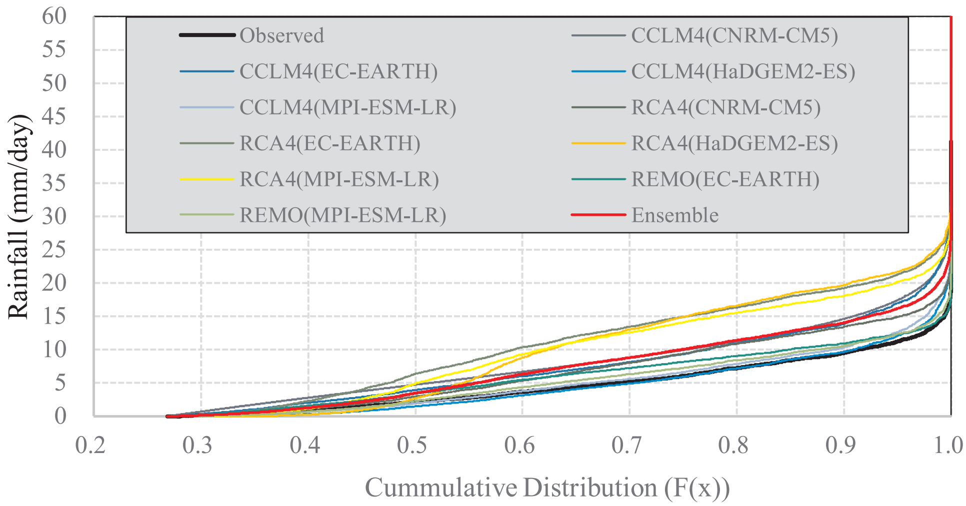

Fig. 5. Cumulative Distribution of RCMs and Observed Daily Rainfall. The values of both observed and RCMs are areal rainfall.

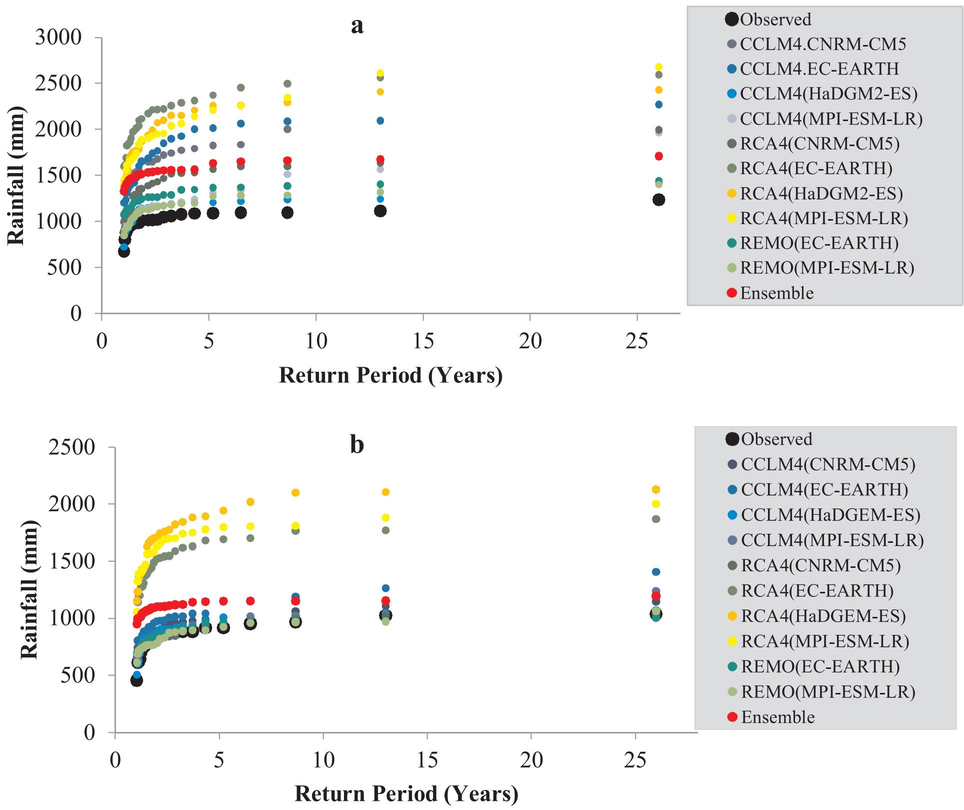

Fig. 6. Observed and RCMs annual (a) and summer (b) rainfall return periods. The values of both observed and RCMs are areal rainfall.

provide more than 600 mm/month rainfall during JJAS season (Fig. 3). However, the observed monthly rainfall was less than 300 mm/month during the JJAS season. Moreover, there was more number of very heavy rainfall events (20 mm/day) in the RCA4 model family than other models (Fig. 5). The results from the RCA4 model family suggests there could be frequent flooding and soil erosion problems which may affect social and ecological systems.

3.3. Statistical evaluation of Regional Climate Models

Statistical metrics (Correlation, BIAS and RMSE) between the areal averaged observed and RCMs rainfall confirmed the difference

Table 3
Correlation, BIAS and RMSE between Observed and RCMs annual and summer rainfall in Jemma sub-basin over 1981–2005.

	Average Rainfall (mm)		CV (%)		Correlation (r)		Bias (%)		RMSE (mm)	
	Annual	JJAS	Annual	JJAS	Annual	JJAS	Annual	JJAS	Annual	JJAS
Observed	1001	815	10.76	16.31	–	–	–	–	–	–
CCLM4(CNRM-CM5)	1631	903	15.95	12.81	0.12	−0.06	62.90	10.8	692	213
CCLM4(EC-EARTH)	1664	977	18.80	16.54	0.19	0.00	66.20	19.9	751	268
CCLM4(HaDGEM2-ES)	1097.	860	13.54	16.22	0.23	0.04	9.60	5.50	225	191
CCLM4(MPI-ESM-LR)	1177	854	19.25	15.61	0.23	0.04	17.62	4.80	313	215
RCA4(CNRM-CM5)	1357	838	17.85	11.40	0.29	0.28	35.50	2.81	462	170
RCA4(EC-EARTH)	2108	1477	13.07	14.77	0.36	0.19	110.9	81.33	1149	730
RCA4(HaDGM2-ES)	1912	1690	15.92	15.96	0.48	0.30	91.00	100.07	969	936
RCA4(MPI-ESM-LR)	1912	1604	16.72	12.76	0.44	0.31	91.00	96.96	970	830
REMO(EC-EARTH)	1248	847	8.11	11.03	0.34	0.17	24.7	3.98	284	187
REMO(MPI-ESM-LR)	1113	821	12.51	12.74	0.37	0.20	11.1	0.76	204	173
Ensemble	1522	1087	6.15	5.50	0.60	0.50	52.0	33.44	545	315

in the performance of RCMs in capturing annual and JJAS rainfall of the Jemma sub-basin. All RCM models overestimated the annual and JJAS rainfall, but with different magnitude. For instance, wet BIAS in annual rainfall ranged from 9.6% in CCLM4 (HadGEM2-ES) model to 110.9% in RCA4 (EC-EARTH) model. Wet BIAS in JJAS rainfall ranged from 0.76% in REMO (MPI-ESM-LR) model to 100.7% in RCA4 (HadGEM2-ES) model. GCMs downscaled using RCA4 RCM showed better correlation than other RCMs, but higher wet BIAS and higher RMSE compared to other models (Table 3). GCMs downscaled using CCLM4 RCM were poorly correlated with the observed rainfall, but BIAS and RMSE in these RCMs were better than RCA4 model family. The outputs of GCMs downscaled using REMO RCM showed better performance in BIAS, RMSE and Correlation compared to RCA4 and CCLM4 model families and the ensemble mean. REMO (MPI-ESM-LR), REMO (MPI-ESM-LR), CCLM4 (HadGEM2-ES) and CCLM4 (MPI-ESM-LR) showed better performance in BIAS, RMSE, and correlation metrics compared to other RCMs.

The ensemble mean of RCMs was superior in correlation metric which shows higher correlation with observed annual and JJAS rainfall than other individual RCM (Table 3). The ensemble mean was also characterized by low coefficient of variation (CV) in relation to the observed rainfall. In CCLM4 and REMO model family, the BIAS and RMSE of JJAS rainfall was better than annual rainfall. While in RCA4 models, poor performance in BIAS and RMSE was observed in the JJAS due to overestimation of JJAS rainfall (Table 3).

3.4. Associations between Sea surface temperature and rainfall of Regional Climate Models

It is investigated that increase in SST in Indian ocean and Equatorial Pacific regions triggers export of dry air from these oceanic regions toward the central highlands of Ethiopia and the Blue Nile River Basin, which further result a decrease in rainfall (Williams et al., 2012; Abtew et al., 2009; Taye and Willems, 2012; Endris et al., 2016). The observed rainfall of the Jemma sub-basin also showed an association with NINO 3.4 index (Table 4). Concurrently, this study showed the teleconnection between SST of CMIP5 GCMs and rainfall of RCMs over the Jemma sub-basin, although not statistically significant. Annual (90%) and JJAS (80%) rainfall of RCMs have negative correlations with GCMs' SST of Pacific Ocean (NINO3.4). The annual (60%) and JJAS (70%) rainfall RCMs also showed negative but weak association with GCMs' SST of Indian ocean (IOD) (Table 4). Simulation of SST (NINO3.4) from some CMIP5 GCMs (HadGEM2-ES and EC-EARTH) showed better correlation with the rainfall of RCMs.

Table 4
Correlation between SST indices and annual and seasonal RCMs rainfall of Jemma sub-basin.

	NINO3.4		IOD	
	Annual	JJAS	Annual	JJAS
Observed	**−0.48**	**−0.37**	–	–
CCLM4(CNRM-CM5)	−0.31	−0.10	−0.00	−0.23
CCLM4(EC-EARTH)	−0.20	−0.03	−0.25	−0.13
CCLM4(MPI-ESM-LR)	−0.15	−0.17	0.15	0.25
CCLM4(HaDGEM2-ES)	−0.37	−0.25	0.14	0.10
CCLM4(HaDGEM2-ES)	−0.37	−0.25	0.14	0.10
RCA4(CNRM-CM5)	−0.03	0.03	−0.03	−0.09
RCA4(EC-EARTH)	−0.32	−0.43	−0.04	−0.11
RCA4(HaDGEM2-ES)	0.39	0.54	−0.25	−0.23
RCA4(MPI-ESM-LR)	−0.14	−0.15	−0.30	0.14
REMO(EC-EARTH)	−0.31	−0.21	0.30	−0.17
REMO(MPI-ESM-LR)	−0.12	−0.23	0.05	0.24

Other studies evaluated the performance of CMIP5 GCMs in simulating the teleconnections between the rainfall and SST in the Blue Nile River Basin, Ethiopian highlands and different regions of Africa. RCMs (CCLM4, RCA4 and REMO) driven by Re-Analysis (ERA-Interim) reasonably simulated the teleconnection between the rainfall and ENSO indices in the Ethiopian highlands (Endris et al., 2013). Zaroug et al., 2014 studied that RegCM4 model driven by reanalysis data showed modest performance in simulating ENSO related rainfall variability in the Upper Blue Nile Basin. In contrast, Bhattacharjee and Zaitchi (2015) were not able to represent any teleconnection between observational based ENSO indices and CMIP5 GCMs rainfall in the Upper Blue Nile Basin. Over Africa, CMIP5 GCMs (MPI-ESM-LR, CNRM-CM5 and HadGEM2-ES) showed overestimation of SST in Guinea Gulf and the West coast of sub-equatorial Africa (Brands et al., 2013). The inability to represent SST by GCMs could be attributed to the fact that CMIP5 GCMs are sensitive to initial conditions, a quasi-equilibrium control run (Taylor et al., 2012). The historical run of CMIP5 GCMs is initiated from an arbitrary point rather than using observed SST data which is the case for Atmospheric models (AMIP). As a result, it is not expected that models simulations to occur at the same time as the observational record.

4. Conclusion

This study showed that the impact of RCMs was stronger than the initial boundary conditions (GCMs) in characterizing the rainfall climatology of the Jemma sub-basin. The outputs of GCMs were downscaled using RCMs, and it was found that GCMs downscaled using REMO and CCLM4 RCMs perform better in representing the annual and monthly rainfall climatology and distribution of rainfall events. When it comes to the areal-average rainfall across the entire sub-basin, all RCMs have shown a positive bias in annual and JJAS rainfall, but with different magnitude. The RCA4 models showed the poorest performance in most of the criteria studied. They showed higher overestimation of annual and JJAS rainfall in the higher altitudes of the sub-basin and higher underestimation in the lower elevation areas of the sub-basin. Higher BIAS, RMSE and extreme rainfall events were also estimated in the RCA4 model family. In terms of capturing the teleconnections with SST, most RCMs rainfall showed negative association, but weak with SST of parent GCMs over the equatorial Pacific and Indian Ocean. This is similar to other studies (Abtew et al., 2009; Taye and Willems, 2012; Williams et al., 2012) that found the negative teleconnection between SST and rainfall of the Blue Nile Basin and Ethiopian Highlands.

Flato et al. (2013) and Kim et al. (2014) found that ensemble mean model outputs represent observed rainfall better than any of the individual RCMs. Likewise, this study showed that mean ensemble output was better in capturing monthly pattern of rainfall than any of the individual RCMs (S-RCM) (Teutschbein and Seibert, 2010). Moreover, the ensemble mean rainfall output showed better correlation with observed annual and JJAS season rainfall. It also showed low variability of rainfall compared to the S-RCM. However, higher overestimation of rainfall, particularly by RCA4 models triggers ensemble mean of RCMs to show weak performance in RMSE and BIAS metrics and in reproducing distribution of rainfall events. Due to the presence of drizzle rainfall events in individual RCMs, there are lower numbers of dry days (0 mm/day) in the ensemble mean of RCMs compared to individual (S-RCM) rainfall events distribution.

In assessment of future climate change impact and adaptation decisions, it is pertinent to identify climate model outputs which can reproduce the climate of the region under study. It is assumed climate modeling schemes which perform well for the current climate are more likely to perform well for future climate conditions (Teutschbein and Seibert, 2012). In our study, the difference in RCMs' ability in simulating current rainfall climatology of the Jemma sub-basin is investigated. The magnitude of biases and distribution of rainfall events was relatively better in REMO and CCLM4 models simulations. The existing biases and differences in capturing distribution of rainfall events in REMO and CCLM4 models can be improved by using statistical bias correction methods and could be satisfactorily used for climate change adaptation decision support systems.

Acknowledgement

This study was made possible through financial support to the first author from Addis Ababa University and the Water and Land Resources Centre (WLRC) of Ethiopia. We are especially indebted to the Ethiopian National Meteorological Agency that kindly provided the daily weather data for this study. We would also like to express our gratitude to the editor and anonymous reviewers for their valuable comments and suggestions.

References

Abtew, W., Melesse, A., Dessalegne, T., 2009. El Ni˜ no Southern Oscillation link to the Blue Nile River Basin hydrology. Hydrol. Process. 23, 3653–3660.
Ali, Y., Crosato, A., Mohamed, Y., Abdalla, S., Wright, N., 2014. Sediment balances in the Blue Nile River Basin. International J. Sediment. Res. 29, 1–13.
Baldauf, M., Seifert, J., Förstner, D., Majewski, M., Raschendorfer, Reinhardt, T., 2011. Operational convective-scale numerical weather prediction with the COSMO model: description and sensitivities. Monthly Weather Rev. 139 (12), 3887–3905. http://dx.doi.org/10.1175/MWR-D-10-05013.1.
Bhattacharjee, P., Zaitchi, B., 2015. Perspectives on CMIP5 model performance in the Nile River headwaters regions. Int. J. Climatol. 35, 4262–4275.
Brands, S., Herrera, S., Fernández, J., Gutiérrez, J., 2013. How well do CMIP5 earth system models simulate present climate conditions in Europe and Africa? Clim Dynam 41 (3–4), 803–817. http://dx.doi.org/10.1007/s00382-013-1742-8.
Buuren, S., Groothuis-Oudshoorn, K., Robitzsch, A., Vink, G., Doove, L., Jolani, S., 2015. Package 'mice' Version 2.25; Multivariate Imputation by Chained Equations.
Diro, G., Grimes, D., Black, E., 2011. Teleconnections between Ethiopian summer rainfall and sea surface temperature: part I—observation and modeling. Clim Dyn 37 (1–2), 103–119.
Dosio, A., Panitz, H., Schubert-Frisius, M., Lüthi, D., 2015. Dynamical downscaling of CMIP5 global circulation models over CORDEX Africa with COSMO CLM: evaluation over the present climate and analysis of the added value. Clim Dyn 44http://dx.doi.org/10.1007/s00382-014-2262-x. 2637–266.
Edwards, P., 2010. History of climate modeling. WIREs Clim Change2011 2, 128–139.
Endris, H., Omondi, P., Jain, S., Lennard, C., Hewitson, B., Chang'a, L., Awange, D., Dosio, A., Ketiem, P., Nikulin, G., Panitz, H., Büchner, M., Stordal, F., Tazalika, L.,

2013. Assessment of the performance of CORDEX regional climate models in simulating East African rainfall. J. Clim. 26, 8453–8475.
Endris, H., Lennard, C., Hewitson, B., Dosio, A., Nikulin, G., Panitz, H., 2016. Teleconnection responses in multi-GCM driven CORDEX RCMs over Eastern Africa. Clim. Dyn. 46, 2821–2846.
Feser, F., Rockel, B., von Storch, H., Winterfeldt, J., Zahn, M., 2011. Regional climate models add value to global model data: a review and selected examples. Bull. Am. Meteorol. Soc. 92 (9), 1181–1192.
Flato, G., Marotzke, J., Abiodun, B., Braconnot, P., Chou, S., Collins, W., Cox, P., Driouech, F., Emori, S., Eyring, V., Forest, C., Gleckler, P., Guilyardi, E., Jakob, C., Kattsov, V., Reason, C., Rummukainen, M., 2013. Evaluation of climate models. Climate Change 2013: The Physical Science Basis. Contribution of Working Group I to the Fifth Assessment Report of the Intergovernmental Panel on Climate Change.
Giorgi, F., Jones, C., Asrar, G., 2009. Addressing Climate Information Needs at the Regional Level: the CORDEX Framework.
Gissila, T., Black, E., Grimes, D., Slingo, J., 2004. Seasonal forecasting of the Ethiopian summer rains. Int. J. Climatol. 24, 1345–1358.
Gleckler, P., Taylor, K., Doutriaux, C., 2008. Performance metrics for climate models. J. Geophys. Res. http://dx.doi.org/10.1029/2007JD008972.
Haile, A., Rientjes, T., 2015. Evaluation of regional climate model simulations of rainfall over the Upper Blue Nile Basin. Atmos. Res. 161–162, 57–64.
Herna′ndez-Diaz, L., Laprise, L., Sushama, L., Martynov, A., Winger, K., Dugas, B., 2013. climate simulation over CORDEX Africa domain using the fifth-generation Canadian Regional Climate Model (CRCM5). Clim Dyn 40, 1415–1433.
Hill, C., Deluca, C., Balaji, Suarez, M., Silva, A., 2009. The Architecture of the Earth System Modeling Framework.
IPCC, 2013. In: Stocker, T.F., Qin, D., Plattner, G.-K., Tignor, M., Allen, S.K., Boschung, J., Nauels, A., Xia, Y., Bex, V., Midgley, P.M. (Eds.), Climate Change 2013: The Physical Science Basis. Contribution of Working Group I to the Fifth Assessment Report of the Intergovernmental Panel on Climate Change. Cambridge University Press, Cambridge, United Kingdom and New York, NY, USA 1535 pp.
Jacob, D., Baerring, L., Christensen, O., Christensen, J., de Castro, M., Deque, M., Giorgi, F., Hagemann, S., Hirschi, M., Jones, R., Kjellstroem, E., Lenderink, G., Rockel, B., Sanchez, E., Schaer, C., Seneviratne, S., Somot, S., van Ulden, A., van den Hurk, B., 2007. An inter-comparison of regional climate models for Europe: model performance in present-day climate. Clim Change 81, 31–52.
Jury, M., 2015. Statistical evaluation of CMIP5 climate change model simulations for the Ethiopian highlands. Int. J. Climatol. 35 (1), 37–44.
Kim, J., Waliser, D.E., Mattmann, C.A., Goodale, C.E., Hart, A.F., Zimdars, P.A., Crichton, D.J., Jones, C., Nikulin, G., Hewitson, B., Jack, C., Lennard, C., Favre, A., 2014. Evaluation of the CORDEX Africa multi-RCM hindcast: systematic model errors. Clim. Dyn. 1189–1202. http://dx.doi.org/10.1007/s00382-013-1751-7.
MoA (Ministry of Agriculture), 2000. Agroecological Zonations of Ethiopia. Addis Ababa, Ethiopia.
Nikulin, G., et al., 2012. Precipitation climatology in an ensemble of CORDEX-Africa regional climate simulations. J. Climate 25, 6057–6078.
Randall, D., Wood, R., Bony, S., Colman, R., Fichefet, T., Fyfe, J., Kattsov, V., Pitman, A., Shukla, J., Srinivasan, J., Stouffer, Sumi, A., Taylor, K., 2007. Climate models and their evaluation. Climate Change 2007: The Physical Science Basis. Contribution of Working Group I to the Fourth Assessment Report of the Intergovernmental Panel on Climate Change.
R Development Core Team, 2015. R: A Language and Environment for Statistical Computing. R Foundation for Statistical Computing, Vienna.
Rowell, D., 2013. Simulating SST teleconnections to Africa: what is the State of the art? J. Clim. 26, 5397–5418.
Saji, N., Goswami, B., Vinayachandran, P., Yamagata, T., 1999. A dipole mode in the tropical Indian Ocean. Nature 401, 360–363.
Samuelsson, P., Jones, C., Wille′n, U., Ullerstig, A., Gollvik, S., Hansson, U., Jansson, C., Kjellström, E., Nikulin, G., Wyser, K., 2011. The Rossby centre regional climate model RCA3: model description and performance. Tellus 63A (63), 4–23.
Seleshi, Y., Zanke, U., 2004. Recent changes in rainfall and rainy days in Ethiopia. Int. J. Climatol. 24, 973–983. http://dx.doi.org/10.1002/joc. 1052.
Taye, M., Willems, P., 2012. Temporal variability of hydroclimatic extremes in the Blue Nile Basin. Water Resour. Res. 48, W03513. http://dx.doi.org/10.1029/2011WR011466.
Taylor, K., Stouffer, R., Meehl, G., 2012. An overview of CMIP5 and the experiment design. Bull. Am. Meteorol. Soc. 93 (4), 485–498. http://dx.doi.org/10.1175/BAMS-D-11-00094.
Teutschbein, C., Seibert, J., 2010. Regional climate models for hydrological impact studies at the Catchment scale: a review of recent modeling strategies. Geogr. Compass 4/7, 834–860.
Teutschbein, C., Seibert, J., 2012. Bias correction of regional climate model simulations for hydrological climate change impact studies: review and evaluation of different methods. J. Hydrol. 456457, 12–29.
Theissen, A., 1911. Precipitation averages for large areas. Monthly Weather Rev. 39, 1082–1084.
Turrado, C., López, M., Lasheras, F., Gómez, B., Rollé, J., Juez, F., 2014. Missing data imputation of solar radiation data under different atmospheric conditions. Sensors 14, 20382–20399. http://dx.doi.org/10.3390/s141120382.
USAID, 2014. A Review of Downscaling Methods for Climate Change Projections. African and Latin American Resilience to Climate Change (ARCC).
Varis, O., Kajander, T., Lemmelä, R., 2004. Climate and water: from climate models to water resources management and vice versa. Clim. Change 66, 321–344.
Viste, E., Sorteberg, A., 2011. Moisture transport into the Ethiopian highlands. Int. J. Climatol. 33, 249–263.
Williams, P., Funk, C., Michaelsen, J., Rauscher, S., Robertson, I., Wils, T., Koprowski, M., Eshetu, Z., Loader, N., 2012. Recent precipitation trends in the Greater Horn of Africa and the emerging role of Indian Ocean sea surface temperature. Clim. Dyn. 39, 2307–2328.
WMO (World Meteorological Organization) 2009. Guidelines on: analysis of extremes in a changing climate in support of informed decisions for adaptation. Climate Data and Monitoring WCDMP-No. 72.
Yilma, A., Awulachew, S., 2009. Characterization and Atlas of the Blue Nile Basin and its Sub-basins. International Water Management Institute.
Zaroug, A., Eltahir, E., Giorgi, F., 2014. Droughts and floods over the upper catchment of the Blue Nile and their connections to the timing of El Niño and La Niña events. Hydrol. Earth Syst. Sci. 18, 1239–1249.
Zhang, X., Yang, F., 2004. RClimDex (1.0) User Guide. Climate Research Branch Environment Canada, Downsview (Ontario, Canada).